Restricted Diffusion of Linear and Star-Branched Polyisoprenes in Porous Membranes

Michael P. Bohrer*

AT&T Bell Laboratories, Murray Hill, New Jersey 07974

Lewis J. Fetters

Exxon Research and Engineering Co., Corporate Research—Science Laboratory, Annandale, New Jersey 08801

Nino Grizzuti†

University of Minnesota, Department of Chemical Engineering and Materials Science, Minneapolis, Minnesota 55455

Dale S. Pearson‡

Exxon Research and Engineering Co., Corporate Research—Science Laboratory, Annandale, New Jersey 08801

Matthew V. Tirrell

University of Minnesota, Department of Chemical Engineering and Materials Science, Minneapolis, Minnesota 55455. *Received January 30, 1987*

ABSTRACT: The flux of linear and star-branched polyisoprene through microporous membranes was measured in order to determine the role of molecular structure in hindered diffusion. As the radius of the pore approached the hydrodynamic radius of the polymer, the effective diffusion coefficient decreased. The reduction for the star-branched polymers was much larger than for the linear polymers. The magnitude of the decrease did not agree with a theoretical model that combined the pore partition coefficient of random flight chains with the hydrodynamic resistance of hard spheres. However, the data correspond qualitatively with recent results on size exclusion chromatography of branched polymers.

Introduction

The effective diffusivity of a polymer within a pore is frequently found to be less than its value in free solution. This phenomenon, known as hindered or restricted diffusion, is caused by two factors, both of which become important when the size of the polymer is comparable to that of the pore through which it passes.

The first factor that reduces diffusivity is the increase in hydrodynamic drag on the polymer caused by the presence of the pore wall. In free solution, the drag is described by the molecular friction coefficient (ζ_0) which is related to the free solution diffusion coefficient (D_0) according to the Einstein equation:

$$D_0 = kT/\zeta_0 \tag{1}$$

where k is Boltzmann's constant and T is temperature. For the case of a solid sphere, the familiar Stokes–Einstein equation, $\zeta_0 = 6\pi\eta_s r$, relates ζ_0 to the radius, r, and the solvent viscosity, η_s. For polymers, a rearranged Stokes–Einstein equation serves to define the hydrodynamic radius, r_H,

$$r_H \equiv kT/6\pi\eta_s D_0 \tag{2}$$

The frictional resistance of objects diffusing through small pores is characterized by a coefficient ζ_P which is larger than ζ_0.

The second factor that reduces the effective diffusivity in a pore is steric exclusion or partitioning. This effect, which is caused by a reduction in the number of configurations allowed to the polymer in the presence of a solid boundary, causes a depleted layer near the pore wall. When the pore size is comparable to the polymer size, this layer extends a constant fraction of the pore radius, r_P. As a result the average equilibrium concentration inside the pore is significantly less than the bulk concentration and there is a concomitant reduction of the diffusion driving force.

In the absence of other specific polymer–wall interactions, such as adsorption, the reduced diffusion in a pore can be expressed as

$$D_P/D_0 = K\,(\zeta_0/\zeta_P) \tag{3}$$

where D_P is the diffusion coefficient through the pore and K is the equilibrium partitioning coefficient, which is equal to the ratio of pore-to-bulk polymer concentration ratio, c_P/c_0. To determine ζ_P, an average of the drag coefficient over all possible polymer configurations inside the pore should be performed. Although such calculations have not been done, it is possible to estimate ζ_P from the simple model of a hard sphere moving along the axis of a cylindrical pore. Values of ζ_P for this case have been obtained numerically by Paine and Scherr.[1]

The commonly used Renkin equation[2] is a form of eq 3 in which the K value for a sphere is combined with approximate hydrodynamic results for spheres obtained by Faxen (cited in ref 3). Faxen's calculations agree well with those of Paine and Scherr up to $r/r_P \simeq 0.4$. Useful discussions of this hydrodynamic-diffusion model for solutes in pores of comparable size can be found in the papers by Bean,[3] Anderson and Quinn,[4] Brenner and Gaydos,[5] and Malone and Anderson.[6]

Quantitative measurements of hindered diffusion rates have been made possible with the development of track-etched membranes of well-defined pore geometry.[7] These membranes, which have generally been made of mica, polycarbonate, or polyester, contain pores of a uniform radius which can be determined independently of the diffusion measurements. Hindered diffusion rates for

† Present address: Department of Chemical Engineering, University of Naples, Naples, Italy.

‡ Present address: Department of Chemical and Nuclear Engineering and Materials Department, University of California at Santa Barbara, Santa Barbara, CA 93106.

0024-9297/87/2220-1827$01.50/0

Table I
Molecular Characteristics of Linear and Star Polyisoprenes

sample	$M_w \times 10^{-4}$	$D \times 10^7$, cm^2/s[a]	r_H, nm[d]	$D \times 10^7$ cm^2/s[e]	r_H, nm[d]	$[\eta]$, cm^3/g	r_η, nm[f]
L-12 (linear)	56.2	13.6,[b] 1.25[c]	18.0, 19.6	1.23	19.9	125	22.3
8-IIIAAAA (8-arm star)	79.5	1.04[b] 1.13[c]	23.5, 21.7			105	23.7
12-IIIAA (12-arm star)	144.0	0.89[b] 0.86[c]	27.6, 28.5	0.92	26.6	127	30.6
18-XAAA (18-arm star)	100.0	1.3,[b] 1.4[c]	18.8, 17.5	1.31	18.8	60	21.2

[a] D obtained by quasi-elastic light scattering. [b] Measurements at Exxon Research and Engineering. [c] Measurements at University of Minnesota. [d] $r_H = kT/6\pi\eta_s D$. [e] D obtained by diffusion through large pores ($r_P = 10$ μm). [f] $r_\eta = [3M[\eta]/10\pi N_{Av}]^{1/3}$.

proteins,[8,9] polysaccharides,[8,10,11] latex particles,[6] and narrow molecular weight polystyrene fractions[12] have been reported. In the present work, track-etched membranes were used to study the effect of molecular structure on diffusivity. In particular, linear and star-branched polyisoprenes synthesized by anionic polymerization techniques were allowed to diffuse through polycarbonate and polyester Nuclepore membranes. The polymers were chosen for this study because of their narrow molecular weight distribution and because high functionality stars are known to behave like hard spheres.[13] In principle, these characteristics should allow us to use simple theories of molecular transport to interpret the data.

Experimental Procedures

A. Polymer Synthesis and Characterization. A detailed procedure for making the type of polymers used in this study has been previously published.[14,15] The description which follows summarizes the essential steps in the method.

Purified isoprene monomer was polymerized at 30 °C in benzene using *sec*-butyllithium as the initiator. When polymerization was complete (~24 h), linear or star-branched polymer was obtained by terminating the poly(isoprenyllithium) with methanol or the appropriate linking agent. For the star-branched polymer, a multifunctional chlorosilane was used as a linking agent. It was added to an excess of polymer lithium, and after 48 h at 50 °C unreacted chain ends were terminated with methanol. The linear polymer resulting from the latter reaction was separated from star-branched material by fractional precipitation. The polymers were dried to a constant weight under vacuum and stored in a refrigerator until used.

The molecular weights of the samples were measured by size exclusion chromatography using a Waters 150 SEC and by time-averaged light scattering using a Sofica PGD, a Fica 50, or a Chromatix KMX-6. The molecular weights so obtained are listed in Table I.

The intrinsic viscosity, $[\eta]$, and self-diffusion coefficient, D, of the samples were measured in *n*-amyl acetate which is the solvent used for the membrane transport experiments. The specific viscosity was determined from the flow times of polymer solutions in Cannon–Ubhelolde capillary viscometers. $[\eta]$ was obtained from this data by extrapolating the specific viscosity divided by concentration to zero concentration (see Table I). It is possible to calculate a characteristic molecular dimension, r_η, from the intrinsic viscosity data by using the equation in footnote *f* of Table I. The values so obtained are in good agreement with r_H determined from D_0 by using eq 2. r_η averages about 11% larger than r_H for polyisoprene;[16,17] conversely, linear and star-shaped polystyrenes exhibit $r_\eta \simeq r_H$ in Θ and good solvent environments.[18-22]

D was measured by quasi-elastic light scattering by using a Malvern photometer and a Langley-Ford correlator[23] (at University of Minnesota) or a Brookhaven Instruments photometer and correlator (at Exxon).[17] Measurements were made at a number of angles, θ, from 30° to 135°, and the decay constant, Γ, of the intensity correlation function $[\langle I(0)I(t)\rangle/\langle I^2\rangle - 1]^{1/2}$ was obtained by fitting the data to a single exponential or a second-order cumulant expansion.[24] The value of Γ obtained by these two methods was essentially the same and proportional to q^2 where $q = 4\pi/\lambda \sin \theta/2$ and λ is the wavelength of light. D values extracted from these measurements ($D = \Gamma/q^2$) were determined at a number of concentrations below c^* ($c^* \simeq 1/[\eta]$) and then linearly extrapolated to $c = 0$ to obtain D_0. Values of D_0 for each of the four polymers studied are listed in Table I.

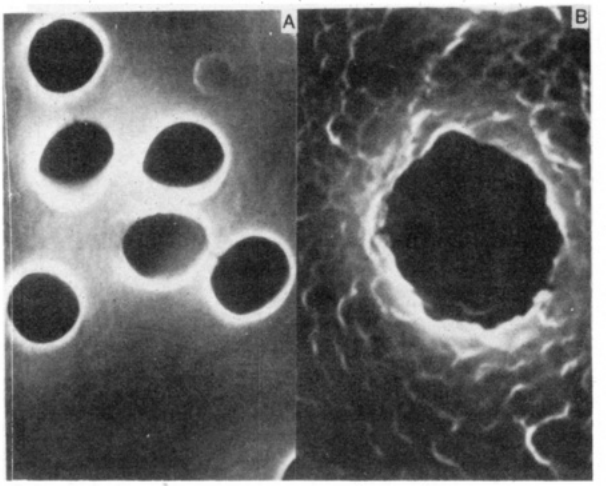

Figure 1. Scanning electron micrographs of track-etched membranes: (A) polycarbonate membrane with 5.0-μm nominal pore diameter (magnification = 1050×); (B) polyester membrane with 10.0-μm nominal pore diameter (magnification = 1050×).

B. Membrane Characterization. Track-etched polycarbonate and polyester membranes with nominal pore diameters of 10.0, 0.2, 0.1, 0.05, and 0.03 μm were obtained from Nuclepore Corp. Scanning electron microscopy reveals that the pores are circular in shape on the surface of the membrane (see Figure 1) and cross-sectional analysis using ultramicrotomy[25] confirms that the pores of polycarbonate membranes are well represented as uniform cylinders. Typical scanning electron microscope photographs of a polycarbonate and a polyester membrane are present in parts A and B of Figure 1, respectively. The surface and edges of the polyester membrane are considerably rougher in appearance than those of the polycarbonate membrane. The membrane thickness was determined from the membrane weight per area by using a value of 1.19 g/cm^3 for the density of polycarbonate and 1.39 g/cm^3 for the density of polyester. Pore length is very nearly equal to membrane thickness, exceeding membrane thickness only to the extent that the pores are not aligned normal to the membrane surface. The maximum deviation from the normal is 29° (information from Nuclepore) which means that average pore length would exceed membrane thickness by 6.8% assuming all deviations of 0–29° to be equally probable. Employing this factor, pore length will be given by

$$L = \frac{1.068W}{(1 - n\pi r_P^2)A\rho} \tag{4}$$

where W is the weight of a membrane of area A, ρ is the density of polycarbonate or polyester, and the denominator includes a correction for membrane porosity ($n\pi r_P^2$). Pore density is given by n and r_P represents the pore radius.

Pore density for each membrane was determined by counting the number of pores in scanning electron microscope photographs obtained at 160–22000× magnification. A minimum of 12 photographs were used to determine the pore density for each membrane lot. The magnification was chosen such that each photograph contained 40–120 pores in an area of 63 cm^2. The membranes were prepared for microscopy by lightly coating with gold and the magnification was calibrated by photographing diffraction gratings of known dimension. For the largest pore size (nominally 5-μm radius), the actual pore radius was deter-

Table II
Average Properties of Polycarbonate and Polyester Membranes

nominal pore diam, μm	type	L, μm	n, cm^{-2}	r_P, nm[a]	$n\pi r_P^2$
10.0	polyester	8.50	1.02×10^5	4848[b]	0.075
0.2	polyester	9.65	3.64×10^8	153	0.267
0.1	polyester	5.97	4.83×10^8	74.3 (65.2)	0.084
0.05	polycarbonate	6.85	6.55×10^8	59.3	0.072
0.03	polycarbonate	6.64	6.79×10^8	43.3 (40.4)	0.040

[a] Determined from flow experiments using n-amyl acetate. Values in parentheses were determined from water flow measurements. [b] Determined from calibrated scanning electron microscope photographs.

mined directly from electron microscope photographs such as the ones shown in Figure 1. Resolution of the pore edge was not adequate to determine pore dimensions for the smaller pore sizes studied. For these membranes, pore radii were determined from measurements of the hydraulic permeability. Flow measurements were performed for each membrane size with the membrane mounted in the diffusion cell (see below), and a calibrated syringe pump was used to pump solvent (n-amyl acetate) or water through the membrane pores. A vertical tube attached to the pump inlet side of the diffusion cell allowed the resulting pressure drop to be measured under steady-flow conditions. Flow rates were chosen to keep the pressure drop across the membrane in the range from 1.3 to 3.5 kPa. The Poiseuille equation was used to interpret the results:

$$Q = r_P^4 \frac{\pi n A}{8\eta L} \Delta P \tag{5}$$

where Q is the volume flow rate, ΔP is the pressure drop, and η is the fluid viscosity. The pore Reynolds number never exceeded 2×10^{-4}. Experiments were performed at room temperature (23 ± 1 °C) and the data from the literature[26] were used to obtain the following values for the density and viscosity of n-amyl acetate at 23 °C: η = 0.767 cP and ρ = 0.731 g/cm^3.

Typically, two or three solvent flow measurements were made on each of the membranes used for diffusion experiments. In addition, for two of the membranes (0.03- and 0.1-μm nominal pore diameter), the pore radii were determined from water as well as n-amyl acetate flow measurements. As indicated in Table II, the values of r_P measure in water were found to be 7 and 12% lower than the values determined with n-amyl acetate. Apparently, the n-amyl acetate only slightly changes the pore dimension of either the polycarbonate or polyester membrane. This is in contrast to the findings of Cannell and Rondelez[12] who measured significantly larger pore radii for polycarbonate membranes with ethyl acetate as compared to water. It may be noted that the measured values of the pore radii are substantially larger than the nominal values (43.3 vs. 15 nm, 59.3 vs. 25 nm, 74.3 vs. 50 nm, and 153 vs. 100 nm) for all but the largest pore size (4840 vs. 5000 nm). Similar discrepancies between nominal and measured pore sizes for these types of membranes have been reported previously.[27]

The average characteristics of the membranes used in this study are summarized in Table II. The uncertainty in the measured values of pore length (L), pore radius (r_P), and pore density (n) is estimated to be ±2%, ±3%, and ±8%, respectively. In general, two or three different membranes from the same lot were used in the diffusion experiments and the average values of the membrane characteristics are the ones reported.

C. Diffusion Measurements. The diffusion cells were made from glass O-ring joint tubes which had been sealed by fusing a circular glass disk to the open ends. Ground-glass joints were connected to the top side of each half of the diffusion cell as illustrated in Figure 2 and plugs with two 18-gauge stainless steel tubes were inserted for sampling. The membrane is supported on its periphery by two annular disks (Teflon) which are clamped between the glass O-ring joints. Ethylene–propylene O-rings are used to seal the membrane and cell compartments as shown in Figure 2. Diffusion experiments were performed at room temperature (23 ± 1 °C) and the cell volume was measured by

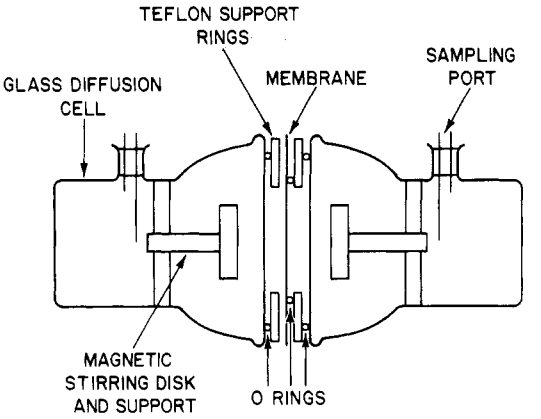

Figure 2. Diffusion cell.

weighing the cell before and after filling with water. Cell volumes were 12.7 mL for one cell, 16.0 mL for three of the cells, and 78.0 mL for a fifth cell. Stirring disks, composed of Teflon-coated magnets, were mounted on stainless steel shafts and held in the diffusion cell by means of a Teflon bracket attached to the membrane holder. An external magnet, coupled to a motor with a tachometer, was used to control the stirring speed. Membrane diffusion coefficients obtained in the larger pore size membranes were found to be strongly influenced by the stirring rate even at speeds as low as 50 rpm. This was taken as evidence of convective driven flow through the membrane due to the stirring. In order to avoid this convection, the experiments reported here were obtained with no stirring. Concentration measurements made before and after stirring the cell at 50 rpm for 5 min were found to be essentially the same, indicating that diffusion of polymer in the solutions on either side of the membrane was much greater than the diffusion rate through the membrane pores.

The difference in concentration between each chamber was recorded periodically by drawing solution from one chamber into the cell of a differential refractive index monitor and recording its refractive index relative to pure solvent. The procedure was repeated for the opposite side and the total time for both measurements was approximately 2 min. Each side of the cell was kept closed at all times except during sampling, to ensure that no pressure-driven flow occurred through the membrane. Conservation of mass for the diffusion cell indicates that the concentration difference (ΔC) between the two chambers is given by

$$\ln [\Delta C_0/\Delta C] = 2At/VR \tag{6}$$

where ΔC_0 is the concentration difference at time $t = 0$, A is the exposed membrane area, V is the cell volume, and R is the total mass transfer resistance. The diffusion coefficient (D_P) of the polymer within the membrane pores is related to R by

$$R = \frac{L}{n\pi r_P^2 D_P} + R_b \tag{7}$$

where the first term on the right-hand side represents the membrane resistance and R_b represents the boundary layer resistance to mass transport on both sides of the membrane as well as a correction for the fact that diffusion is not one dimensional near the membrane surface.[27,28] R_b for each membrane was determined in the present study by measuring the diffusion of isoprene monomer in n-amyl acetate. Since isoprene is much smaller than any of the membrane pore sizes, the value of D_0 could be substituted for D_P in eq 7, thereby permitting R_b to be calculated. As discussed by Colton and Smith,[29] mass transfer coefficients in this geometry follow a correlation of the form

$$A/R_b D_0 \propto Sc^{1/3} \tag{8}$$

where A is the radius of exposed membrane and Sc is the Schmidt number ($\eta/\rho D_0$). This correlation was used to determine the value of R_b for polyisoprene from the measured isoprene R_b values according to

$$R_{b,\text{polyisoprene}} = R_{b,\text{isoprene}} \left[\frac{D_{0,\text{isoprene}}}{D_{0,\text{polyisoprene}}} \right]^{2/3} \tag{9}$$

The free solution diffusion coefficient for isoprene in *n*-amyl acetate was calculated with eq 7 to be 1.37×10^{-5} cm^2/s after measuring its resistance through the 10.0-μm membrane. The value of R_b used in this equation was determined from the total resistance (R) for a substance whose D_0 is known. We used the glucose/water system with the same membrane ($D_0 = 6.73 \times 10^{-5}$ cm^2/s). Finally the value of $R_{b,isoprene}$ is determined from the relationship derived from eq 8

$$R_{b,isoprene} = R_{b,glucose}\left[\frac{D_{0,glucose}}{D_{0,isoprene}}\right]^{2/3}\left[\frac{(\eta/\rho)_{water}}{(\eta/\rho)_{n\text{-amyl acetate}}}\right]^{1/3} \quad (10)$$

The procedure used for the diffusion experiments was similar in each case. Initially, each chamber was filled with solvent, one side was closed off, and approximately 1.0 mL of a polymer solution prepared with *n*-amyl acetate was added to the other side. The slope of a plot of ln $(\Delta C_0/\Delta C)$ vs. t was obtained by linear regression and correlation coefficients usually exceeded 0.99. The time of the experiments varied from about 24 h for the largest pore size membranes to ~14 days for smallest pore size.

Adsorption of the polyisoprene polymers on either type of membrane, an effect which would alter the pore dimension and interfere with the diffusion measurement, was examined by measuring solvent flow rates before and after a 72-h exposure of the smallest pore size membrane to polyisoprene. The pore radius was found to be 42.9 nm initially and 40.4 nm after exposure to a 6.2×10^{-4} g/mL solution of 18-arm star polyisoprene. The finding that pore radius is essentially unchanged is taken as an indication of no polymer adsorption on the membrane material. Further support for this conclusion comes from the observation that the hindered diffusion rates were unchanged over time periods from 1 to 14 days. In contrast, preliminary experiments with cyclohexane as the solvent did show evidence of adsorption, since the measured diffusion coefficients were found to decrease significantly with time of exposure to the polyisoprene solution. Apparently, the polar nature of the *n*-amyl acetate prevents polymer adsorption on the membrane.

The concentration of polymer used in the diffusion experiments was 1.5×10^{-4} to 1.0×10^{-3} g/mL. This is far below the overlap concentration, c^*, which we estimate to be $1/[\eta]$. Under these conditions the hydrodynamic radius of the polymer should be the same as that determined from D_0 using $r_H = kT/6\pi\eta_s D_0$. The values of r_H determined in this way are given in Table I.

Results and Discussion

The results of the diffusion experiments are summarized in Table III where we list the total resistance R, the boundary layer resistance R_b, and the ratios D_P/D_0 and r_H/r_P for five different membranes. The value of R_b is found to be insignificant for the smallest membrane pore size but represents 10, 16, 70, and 67% of the total resistance for the 0.05-, 0.1-, 0.2-, and 10.0-μm membranes, respectively.

The most important result is that the pore diffusivity of all polymers is strongly reduced with respect to the bulk value in all but the largest membrane pore size. The finding that the diffusion coefficients for the 10.0-μm membrane are close to the free solution values determined by quasi-elastic light scattering is a good indication of the validity of our technique for measuring diffusion coefficients.

Our results are also presented in graphical form in Figure 3 where (D_P/D_0) is shown as a function of r_H/r_P. We note that the diffusivity of both linear and branched polymers within the membrane pores is significantly reduced relative to free solution for values of $r_H/r_P > 0.2$, in reasonable agreement with previous findings of others.[8-12,30] The solid curve represents the Renkin equation for solid spheres diffusing along the axis of a cylindrical pore but modified to include the more accurate hydrodynamic data of Paine and Scherr.[1] The linear polymer data fall slightly above this curve and a clear distinction be-

Table III
Polyisoprene Diffusion Data

nominal pore diam, μm	linear polyisoprene				8-arm star polyisoprene				12-arm star polyisoprene				18-arm star polyisoprene			
	R, s/cm	R_b, s/cm	r_H/r_P	D_P/D_0	R, s/cm	R_b, s/cm	r_H/r_P	D_P/D_0	R, s/cm	R_b, s/cm	r_H/r_P	D_P/D_0	R, s/cm	R_b, s/cm	r_H/r_P	D_P/D_0
10.0	285 000	193 000	0.0038	0.94					363 000	242 000	0.057	1.05	271 000	184 000	0.037	0.97
0.2	251 000	221 000	0.12	0.92					59 000	288 000	0.18	0.16	311 000	217 000	0.12	0.28
0.1	248 000	85 800	0.25	0.34	877 000	97 000	0.30	0.084	2040 000	112 000	0.37	0.42	663 000	84 100	0.24	0.091
0.05	376 000	78 300	0.31	0.24	1240 000	88 500	0.38	0.76	2450 000	102 000	0.47	0.046	1010 000	76 700	0.30	0.075
0.03	1190 000	33 200	0.43	0.11	2180 000	37 600	0.52	0.071	3740 000	43 500	0.64	0.051	2920 000	32 600	0.42	0.043

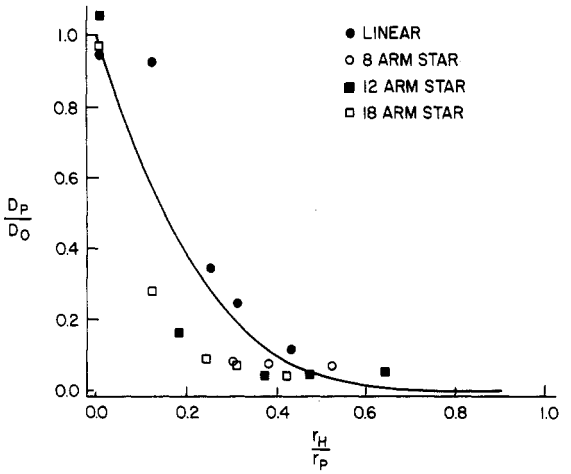

Figure 3. Ratio of the pore-to-bulk diffusivities for linear and star-branched polyisoprenes as a function of the ratio of hydrodynamic radius to pore radius. The solid curve is calculated from eq 3 by using K values for rigid spheres and frictional coefficients from Paine and Scherr.[1]

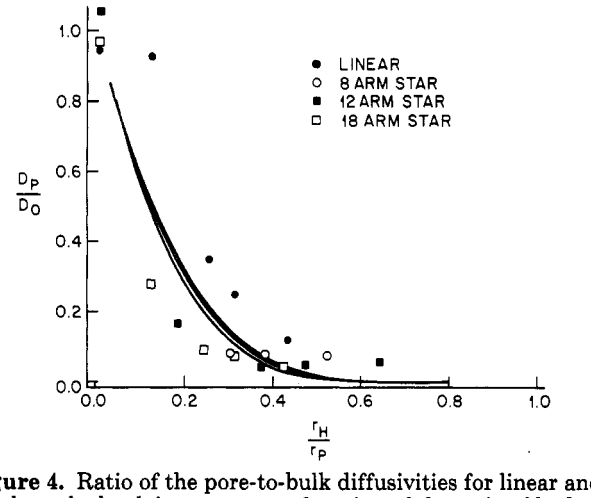

Figure 4. Ratio of the pore-to-bulk diffusivities for linear and star-branched polyisoprenes as a function of the ratio of hydrodynamic radius to pore radius. The solid curves are calculated from eq 3 by using Casassa's K values (eq 12) for linear, 8-arm star, 12-arm star, and 18-arm star polymers, and frictional coefficients from Paine and Scherr.[1] At $r_H/r_P = 0.3$, the curve for linear polymers is at the bottom, 18-arm stars in the middle, and 8- and 12-arm stars superposed at the top.

tween linear and star-branched polymers is seen: at fixed r_H/r_P the branched polymers all lie well below the data for linear polymer.

As previously pointed out, the reduction in diffusivity of the solute is due to two factors: the partitioning effect which reduces the polymer concentration in the pore and the frictional effect caused by hydrodynamic interactions between the polymer and the wall. The former effect has been analyzed for random flight chains including star-shaped polymers by Casassa[31] and Casassa and Tagami.[32] However, a rigorous treatment of the frictional effect is not available to combine with their calculated values of K.

Daoud and de Gennes[33] and Brochard and de Gennes[34] have presented scaling arguments that treat both aspects of the problem. A brief review is given in the Appendix. Their analyses are useful not only for the inclusion of frictional effects but because they also deal with good solvent effects which were not included in previous calculations.[17,23] However, the results are only qualitative because they contain unknown constants and because their predictions for the weak confinement region $r_H < r_P$ where experiments are done are based entirely on the expected behavior in the strong confinement region $r_H \gg r_P$. For practical reasons free diffusion data cannot be obtained in the strong confinement region because the flux is too low (see Figure 3).

In the analysis to follow we decided it was more appropriate to combine Casassa's results for random flight polymers with the hydrodynamic results for spheres. The following aspects of our experiment seem to justify this combination: (1) *n*-amyl acetate is only a marginal solvent for polyisoprene and hence random statistics should be approximately correct and (2) previous work by Roovers[13] suggests that high functionality stars approach hard spheres in their hydrodynamic behavior.

Casassa and Tagami[32] calculated the partition coefficients of linear and star-shaped polymers in different pore geometries. A star molecule is assumed to be formed of f random walks starting at the same point. The statistics of each walk is governed by the diffusion equation[31]

$$\frac{\partial P_n(\mathbf{r})}{\partial n} = \frac{b^2}{6}\nabla^2 P_n(\mathbf{r}) \tag{11}$$

where b is average step length and $P_n(\mathbf{r})\,d\mathbf{r}$ is the probability of finding the nth step of a walk that begins at the origin in the volume element between $\mathbf{r}$ and $\mathbf{r} + d\mathbf{r}$. To account for the presence of the pore, an absorbing boundary condition is used such that any configuration which touches the wall is eliminated. Their analysis of cylindrical pores gives the following expression for the ratio of the pore concentration to the bulk concentration:

$$K = 2^{f+1}\int_0^1 \left[\sum_{j=1}^{\infty}\frac{1}{\alpha_j}\exp\left[-\frac{(\alpha_j r_G/r_P)^2 f}{3f-2}\right]\frac{J_0(\alpha_j t)}{J_1(\alpha_j)}\right]^f t\,dt \tag{12}$$

where r_G is the radius of gyration of the polymer, α_j are the positive roots of $J_0(\alpha_j) = 0$, and J_0 and J_1 are Bessel functions of the first kind of order zero and one.[35] The mean-square radius of gyration of a random flight star-branched polymer is given by

$$\langle r_G^2\rangle = \frac{Nb^2}{6}\frac{3f-2}{f} \tag{13}$$

where N is the number of steps per arm. To compare eq 12 with our data we need to know the relationship between r_G and r_H. Theoretical results for random flight polymers are available but we prefer to use the published data of Roovers et al.[13] They find that r_G/r_H equals 1.29 for linear polymers, 0.81 for 12-arm stars, 0.79 for 18-arm stars, and by interpolation 0.87 for 8-arm stars.

Casassa's partition coefficient can now be combined with the hydrodynamic calculations of Paine and Scherr[1] for hard spheres by using r_H as the radius. The results obtained in this way are shown in Figure 4. At equal r_H/r_P the theoretical values of D_P/D_0 are essentially the same for linear and star polymers. However, the data for the linear polymers fall above these curves and indicate that the characteristic size controlling the pore diffusion is approximately 35% smaller than r_H. Conversely the data on star-shaped polymers fall below this curve except for small values of D_P/D_0 that are on the order of 0.05. The branched polymer data would coincide with the theoretical curves if their characteristic size was approximately 20% larger than the measured r_H.

Comparing our results with data from similar studies using well-defined membranes and other polymer–solvent

systems, considerable differences are noted. For instance, Deen et al.[10] and Bohrer et al.[11] found that values of D_P/D_0 for dextran, a nearly linear polysaccharide, were significantly greater than both the theoretical curve (Renkin equation) and our linear polyisoprene data. On the other hand, those for ficoll, a highly cross-linked polysaccharide, was found to agree quite well with the theoretical curve.[11] Cannell and Rondelez[12] studied linear polystyrene in ethyl acetate with track-etched polycarbonate membranes. Their D_P/D_0 values were significantly lower than the theoretical curve, similar to our findings with star-branched polyisoprenes. It is quite likely that these discrepancies are due to differences in molecular structure or configuration which cause the relationship between measured hydrodynamic radius and steric partitioning or frictional drag to be different among these various polymer–solvent systems. A second possibility is that specific membrane–polymer interactions are contributing to these observed differences. It is unlikely that such interactions are responsible for the difference between linear and star-branched polyisoprenes in the present study, since chemically these polymers are identical.

With both partitioning and frictional factors at work, it is difficult to give a definitive, molecular interpretation to these data. We note, however, that while eq 12 gives a systematic means to calculate how the partition coefficient varies with increasing branching, from the frictional point of view we have treated all of the polymer molecules, linear and branched, as hard spheres with r_H determined from bulk solution data. Since eq 12 has already been shown[31,32] to give a reasonable model of experimental data on partitioning alone and since Figure 4 shows that the effect of arm number through partitioning alone is not a very large factor, it seems reasonable to suggest that it is the hard-sphere model for a linear polymer chain that is most at fault in this 35% discrepancy. It is not clear at this point how to improve on the Paine–Scherr approximation. We note in this regard that de Gennes (ref 36, p 193) has discussed the influence of pore walls on intramolecular hydrodynamic interactions of confined chains. It is clear from that discussion that a confined linear chain may have a smaller effective r_H than its bulk solution value.

A further observation is that all of the branched molecules we studied behave essentially the same, irrespective of arm number. While they are 20% off from the hard sphere, the fact that they all behave similarly suggests that they may all be quite impenetrable to solvent, since they are all quite highly branched.

Our findings appear to be at odds with previous results from size-exclusion chromatography which show that linear and branched molecules of equal hydrodynamic size have equal column elution times.[37] However, more recent studies by Hadjichristidis, Guyot, and Fetters[14] and by Roovers and Toporowski[38] indicate otherwise. These investigators found that star and comb polymers elute from chromatography columns as if their hydrodynamic volumes were larger than the measured ones. Although this trend is in agreement with the work reported here, the differences they observed were not as large (5–10%).[14,38,39]

Summary

It was found that diffusion of flexible polymers through small pores is strongly influenced by the dimensions of the pore. The hindered diffusion coefficient decreases as the polymer-to-pore size ratio increases. The experiments have shown that this effect depends on the structure of the macromolecule: star-branched polymers diffuse through the pores more slowly than linear chains that have the same hydrodynamic radius. It does not seem possible to explain this behavior on the basis of statistics of random flight star-branched polymer chains combined with hydrodynamic drag results for spheres. However, our results are in qualitative agreement with size exclusion chromatography of branched polymer molecules.

Acknowledgment. We gratefully acknowledge the preliminary experimental work of T. A. Woodfield and helpful discussions with J. L. Anderson, M. Davidson, W. M. Deen, and I. Kathawalla.

Appendix

Daoud and de Gennes[33] have presented a scaling method for obtaining the free energy required to confine a polymer in a capillary of radius r_P. Their solution is based on the assumption that there are two characteristic lengths in the problem: r_G, the radius of gyration of a free polymer, and r_P. The value of r_G is related to the degree of polymerization N by[36]

$$r_G \propto bN^{\nu} \tag{A1}$$

where $\nu = {}^1/_2$ in poor (Θ) solvents and $\nu \simeq {}^3/_5$ in good solvents.

The confinement free energy is then described by

$$F_N/kT = h(r_G/r_P) \tag{A2}$$

where the dimensionless function h is expected to have the following limiting behavior

$$h(0) = 0 \tag{A3}$$

$$h(x \gg 1) \sim x^m \tag{A4}$$

The value of m can be determined from the requirement that F_N be an extensive function of N. Solving eq A2 under this constraint leads to $m = 1/\nu$ and, therefore,

$$F_N/kT \propto (r_G/r_P)^{5/3} \qquad r_G > r_P \tag{A5}$$

in good solvents and

$$F_N/kT \propto (r_G/r_P)^2 \qquad r_G > r_P \tag{A6}$$

in Θ solvents. The latter results agrees with the Casassa treatment.[31,32] The partition coefficient, K, can now be related to F_N by

$$K = (C_P/C_0) \propto \exp(-F_N/kT) \tag{A7}$$

The frictional resistance for the chain in a capillary has been derived by Brochard and de Gennes.[34] According to their analysis, a polymer chain confined to a one-dimensional tube has a configuration consisting of a sequence of blobs each with radius r_P. The number of monomers per blob is g where $r_P = bg^{\nu}$ and the length of the chain along the tube axis is then $r_{\parallel} = (N/g)r_P$. This leads to a frictional resistance $\zeta_P = 6\pi\eta_s r_{\parallel}$. Rearranging the above equations, we find that

$$\zeta_0/\zeta_P \propto (r_G/r_P)^{-(1-\nu)/\nu} \tag{A8}$$

Therefore, for good solvents

$$\zeta_0/\zeta_P \propto (r_G/r_P)^{-2/3} \qquad r_G > r_P \tag{A9}$$

and for poor (Θ) solvents

$$\zeta_0/\zeta_P \propto (r_G/r_P)^{-1} \qquad r_G > r_P \tag{A10}$$

The above results derived for linear polymers could easily be adapted to star-branched polymers.[40,41] It should be noted that these formulas were derived by considering the strong confinement limit ($r_G \gg r_P$). Because they are scaling relationships that lack precise coefficients and the details of the crossover behavior leading to the weak

confinement limit ($r_G < r_P$), a quantitative comparison with the results presented here was not attempted.

Registry No. Polyisoprene, 9003-31-0.

References and Notes

(1) Paine, P. L.; Scherr, P. *Biophys. J.* **1975**, *15*, 1087.
(2) Renkin, E. M. *J. Gen. Physiol.* **1954**, *38*, 225.
(3) Bean, C. P. In *Membranes*; Eisenman, G., Ed.; Marcel Dekker: New York, 1972; Vol. 1, p 1.
(4) Anderson, J. L.; Quinn, J. A. *Biophys. J.* **1974**, *14*, 130.
(5) Brenner, H.; Gaydos, L. J. *J. Colloid Interface Sci.* **1977**, *58*, 312.
(6) Malone, D. M.; Anderson, J. L. *Chem. Eng. Sci.* **1978**, *33*, 1429.
(7) Price, P. B.; Walker, R. M. *J. Appl. Phys.* **1962**, *33*, 3407.
(8) Beck, R. E.; Schultz, J. S. *Biochim. Biophys. Acta* **1972**, *255*, 273.
(9) Wong, H. J.; Quinn, J. A. *Colloid Interface Sci.* **1976**, *5*, 169.
(10) Deen, W. M.; Bohrer, M. P.; Epstein, N. B. *AIChE J.* **1981**, *27*, 952.
(11) Bohrer, M. P.; Patterson, G. D.; Carroll, P. J. *Macromolecules* **1984**, *17*, 1170.
(12) Cannell, D. S.; Rondelez, F. *Macromolecules* **1980**, *13*, 1599.
(13) Roovers, J.; Hadjichristidis, N.; Fetters, L. J. *Macromolecules* **1983**, *16*, 214.
(14) Hadjichristidis, N.; Guyot, A.; Fetters, L. J. *Macromolecules* **1978**, *11*, 668.
(15) Bauer, B. J.; Hadjichristidis, N.; Fetters, L. J.; Roovers, J. E. L. *J. Am. Chem. Soc.* **1980**, *102*, 2410.
(16) Tsvetkov, V. N.; Lavrenko, P. N.; Bushin, S. V. *J. Polym. Sci., Polym. Chem. Ed.* **1984**, *22*, 3447.
(17) Davidson, N.; Fetters, L. J.; Funk, W. G.; Hadjichristidis, N.; Graessely, W. W., unpublished results.
(18) Roovers, J.; Toporowski, P. M. *J. Polym. Sci., Polym. Phys. Ed.* **1980**, *18*, 1907.
(19) Nemoto, N.; Makita, Y.; Tsunashima, Y.; Kurata, M. *Macromolecule* **1984**, *17*, 425.
(20) Miyaki, Y.; Einaga, Y.; Fujita, H. *Macromolecules* **1978**, *11*, 1180.
(21) Einaga, Y.; Miyaki, Y.; Fujita, H. *J. Polym. Sci., Polym. Phys. Ed.* **1979**, *17*, 2103.
(22) Khasat, N.; Pennisi, R.; Hadjichristidis, N.; Fetters, L. J. submitted for publication in *Macromolecules*.
(23) Balloge, S.; Tirrell, M. *Macromolecules* **1985**, *18*, 817.
(24) Koppel, D. E. *J. Chem. Phys.* **1972**, *57*, 4814.
(25) Liabastre, A. A.; Orr, C. *J. Colloid Interface Sci.* **1978**, *64*, 1.
(26) *Beilstein, 4th ed.* **1960**, *2*, 247; **1975**, *2*, 152.
(27) Bohrer, M. P. *Ind. Eng. Chem. Fundam.* **1983**, *22*, 72.
(28) Keller, K. H.; Stein, T. R. *Math. Biosci.* **1967**, *1*, 421.
(29) Colton, C. K.; Smith, K. A. *AIChE J.* **1972**, *18*, 958.
(30) Guillot, G.; Leger, L.; Rondelez, F. *Macromolecules* **1985**, *18*, 2531.
(31) Casassa, E. F. *J. Polym. Sci., Polym. Lett. Ed.* **1967**, *5*, 773.
(32) Casassa, E. F.; Tagami, Y. *Macromolecules* **1969**, *2*, 14.
(33) Daoud, M.; de Gennes, P.-G. *J. Phys.* **1977**, *38*, 85.
(34) Brochard, F.; de Gennes, P.-G. *J. Chem. Phys.* **1977**, *67*, 52.
(35) *Handbook of Mathematical Functions*; Abramowitz, M., Stegun, I. A., Eds.; Dover: New York, 1965; Chapter 9.
(36) de Gennes, P.-G. *Scaling Concepts in Polymer Physics*; Cornell University: Ithaca, NY, 1979.
(37) Grubisic, Z.; Rempp, P.; Benoit, H. *J. Polym. Sci., Polym. Lett. Ed.* **1975**, *5*, 753.
(38) Roovers, J.; Toporowski, P. M. *Macromolecules* **1981**, *14*, 1174.
(39) Roovers, J.; Hadjichristidis, N., private communication.
(40) Daoud, M., private communication.
(41) Halpern, A.; Alexander, S. *Macromolecules* **1987**, *20*, 1146.

Hydrophobic Attraction of Pyrene-End-Labeled Poly(ethylene glycol) in Water and Water–Methanol Mixtures

Kookheon Char, Curtis W. Frank,* Alice P. Gast,* and Wing T. Tang

Department of Chemical Engineering, Stanford University, Stanford, California 94305.

Received November 11, 1986

ABSTRACT: Fluorescence stationary-state measurements of pyrene-end-labeled poly(ethylene glycols) (Py-PEG-Py) of three different molecular weights are presented. In aqueous solution the excimer to monomer intensity ratio, I_e/I_m, in the intramolecular excimer region decreases as the polymer molecular weight is increased. For Py-PEG-Py of PEG weight-average molecular weight of 4800, the I_e/I_m does not scale according to the Wilemski–Fixman theory based on a diffusion-controlled end-to-end cyclization process. Surprisingly, this Py-PEG-Py(4800) phase separates. We believe that these observations are due to a hydrophobic attraction between pyrene groups. The addition of methanol reduces the hydrophobic attraction by the preferential solvation of methanol molecules around the pyrene group.

Introduction

Fluorescence techniques have long been employed to investigate the dynamics of chemical species at the molecular level. There is a large amount of literature dealing with the studies of molecular dynamics of either synthetic or natural molecules with the aid of a variety of fluorescence techniques.[1] Among the various fluorescence methods, excimer formation has been frequently used to study polymer dynamics. In this technique an aromatic ring in an electronically excited state must encounter an identical chromophore in the ground state during the lifetime of the excited state. If the two chromophores are in the proper geometry they can form a sandwich-shaped excimer giving a broad emission at a lower energy than that of the individually excited aromatic ring. Examples of the application of excimer formation using probe molecules similar to those examined in this work are in the detection of the formation of association complexes between two different water-soluble polymers[2-4] and as probes of the end-to-end cyclization of polymer chains.[5-8] Among the many possible fluorescent chromophores, pyrene and its derivatives have been extensively used to study excimer formation due to their long excited-state lifetime and their spectral sensitivity to the medium examined.[9] The spectral sensitivity of pyrene molecules to the local environment has been employed to study micelle formation of surfactants or block copolymers[10-12] and polymer adsorption on surfaces.[13-16]

Traditionally, the introduction of fluorescent groups is considered a benign process to study intrinsic properties without perturbing the polymer chains. However, this may not be true for short polymer chains in a particular solvent. Cheung et al.[7] found anomalous behavior in the study of diffusion-controlled end-to-end cyclization using pyrene-end-labeled poly(ethylene glycols) in various solvents. They were able to correlate the measured excimer to monomer intensity ratio, I_e/I_m, with the inverse solvent viscosity in all solvents except water and methanol where

0024-9297/87/2220-1833$01.50/0